Wide Post-Mass Transfer White-Dwarf Binaries

Runqiu Ye

June, 2024

1 Introduction

Common envelope (CE) is the outcome of unstable mass transfer. During CE, both stars orbit inside an envelope and spiral inward. If the energy liberated in this process is enough to eject the CE, then the result of CE process is a close binary. If, on the contrary, the liberated energy is not enough to eject the envelope, then the result of the process is a merger. In observation results, a number of WD+MS binaries are wider than expected, and CE is expected to be the main channel to form these white dwarf binaries [Yamaguchi et al., 2024a, Yamaguchi et al., 2024b]. In the MESA model utilized by [Yamaguchi et al., 2024a, Yamaguchi et al., 2024b], wide post-CE WD+MS binaries can be formed in a certain range of initial separation with only gravitational and internal energy included in the calculation.

In this paper, we are going to explore the formation possibility of these wide post-mass transfer WD+MS binaries with COSMIC model. We perform COSMIC simulation on both individual binary star systems and sampled population to explore the formation of WD+MS binaries under different conditions. In section 2, we are going to investigate formation of individual wide WD+MS binaries through CE for a variety of variables, including initial mass, initial separation, CE efficiency, and the energy budget of the CE. In section 3, we are going to explore the formation of individual wide WD+MS binaries through stable mass transfer. In section 4, we will research on how different COSMIC model affect simulation results of a sample population of binary star systems, and how the formation of post WD+MS binaries depends on various parameters.

Throughout the paper, the stellar type and evolution type follows the BSE conventions. `kstar` values specify the evolutionary state of the star, and `evol_type` values specify the evolutionary changes of the binary systems:

kstar	evolutionary state	evol_type	evolutionary change
0	MS $< 0.7\,\mathrm{M}_\odot$	1	initial state
1	MS $> 0.7\,\mathrm{M}_\odot$	2	kstar change
2	Hertzprung Gap	3	begin Roche lobe overflow
3	First Giant Branch	4	end Roche lobe overflow
4	Core Helium Burning	5	contact
5	Early AGB	6	coalescence
6	TP-AGB	7	begin common envelope
7	Naked Helium Star MS	8	end common envelope
8	Naked Helium Star Hertzprung Gap	9	no remnant leftover
9	Naked Helium Star Giant Branch	10	max evolution time
10	Helium White Dwarf	11	binary disruption
11	Carbon/Oxygen White Dwarf	12	begin symbiotic phase
12	Oxygen/Neon White Dwarf	13	end symbiotic phase
13	Neutron Star	14	blue straggler
14	Black Hole	15	supernova of primary
15	Massless Remnant	16	supernova of secondary

2 Formation Through Common Envelope

In [Yamaguchi et al., 2024a, Yamaguchi et al., 2024b], the author discussed the formation of WD+MS binaries through CE for both high-mass and low-mass systems, and it was found that wide WD+MS systems can be formed for certain energy budgets and certain initial separation in the MESA model. We hope to explore similar models in COSMIC.

In [Yamaguchi et al., 2024a, Yamaguchi et al., 2024b], to explore the dependency of the final separation a_f in the post-CE binary on the initial separation a_i in the pre-MT binary, the author first ran a stellar evolution model of the primary star using MESA. Its evolution up to AGB phase is followed. With the model, the binding energy of the CE is calculated as

$$E_{\mathrm{bind}} = E_{\mathrm{grav}} + E_{\mathrm{int}} = \int_{M_{\mathrm{core}}}^{M_{\mathrm{tot}}} -\frac{Gm}{r(m)} + U(m)dm, \tag{1}$$

or

$$E_{\mathrm{bind}} = E_{\mathrm{grav}} + \alpha_{\mathrm{th}} E_{\mathrm{th}} + \alpha_{\mathrm{rec}} E_{\mathrm{rec}}. \tag{2}$$

After that, the change of separation through CE evolution is calculated using

$$E_{\mathrm{bind}} = \alpha_{\mathrm{CE}} \left(-\frac{GM_{\mathrm{WD}} M_\star}{2a_f} + \frac{GM_i M_\star}{2a_i} \right). \tag{3}$$

In COSMIC, the CE is modeled using a structural parameter λ, where

$$E_{\mathrm{bind}} = \frac{GM_i M_{\mathrm{env}}}{\lambda R_i}. \tag{4}$$

This λ is represented in COSMIC as the `lambdaf` flag in `BSEDict`. To compare MESA model with COSMIC, we intend to compare how the energy budget utilized in past papers matches with the CE model in COSMIC. We approach this by calculating the effective λ value for each of the common envelope energy budget used in [Yamaguchi et al., 2024a, Yamaguchi et al., 2024b].

2.1 High Mass Systems ($7\,\mathrm{M}_\odot + 1\,\mathrm{M}_\odot$)

2.1.1 Methods and results

According to [Yamaguchi et al., 2024a], the lower limit of WD mass $M_{\mathrm{MD,min}}$ in the observational sample is calculated to be $1.244\,\mathrm{M}_\odot \sim 1.418\,\mathrm{M}_\odot$. The corresponding mass of MS progenitor is expected to be in the range of $6 \sim 9\,\mathrm{M}_\odot$, and the companion mass has median around $1\,\mathrm{M}_\odot$. MESA results for $7\,\mathrm{M}_\odot+1\,\mathrm{M}_\odot$ systems is documented in [Yamaguchi et al., 2024a]. Hence, we also consider a $7\,\mathrm{M}_\odot + 1\,\mathrm{M}_\odot$ evolution model in COSMIC and compare the results with those in [Yamaguchi et al., 2024a].

We ran COSMIC binary evolution simulation of a $7\,\mathrm{M}_\odot + 1\,\mathrm{M}_\odot$ system and investigate how the final separation a_f depends on the initial separation a_i and the CE parameter λ. The initial separation is a linear grid in range $2 \sim 8\,\mathrm{au}$ with 400 points. The CE flag `lambdaf` is a linear grid in range $0 \sim -100$ with 2000 steps, which corresponds to $0 \sim 100$ for CE parameter λ. Also, we ran these parameters with four different CE efficiencies — $\alpha_{\mathrm{CE}} = 1$, $\alpha_{\mathrm{CE}} = 0.9$, $\alpha_{\mathrm{CE}} = 0.6$, and $\alpha_{\mathrm{CE}} = 0.3$, the same as recorded in [Yamaguchi et al., 2024a]. In total, for each of the 4 different CE efficiency α_{CE}, we ran a grid of 80000 binary star systems with different initial separation a_i and CE parameter λ.

After simulation is finished, we select the time-step when the system finished CE for the first time (`evol_type = 8`). At this moment, if the system is a WD+MS system, we record their separation as the final separation a_f. Otherwise, we set $a_f = 0$ and consider this initial condition unable to produce a WD+MS system. We create four heat maps for the four different CE efficiencies. In Figure 1, we plot the final separation a_f of the WD+MS systems against initial separation a_i and the CE flag $-\lambda$.

2.1.2 Discussions

There are several interesting points of the results. First of all, comparing the four panels, we found that as α_{CE} decreases, the final separation decreases in general. This can be explained by Equation 3. Qualitatively, note that more energy from the orbit is needed to eject the envelope for low α_{CE}, so the resulting a_f is expected to be smaller.

It is worth noting that most of these systems experience two mass transfer phases in COSMIC before reaching WD+MS. That is, during the evolution process, two CE processes take place, between which there is a period of time. A typical change of `evol_type` through the evolution is **...-3-7-8-4-...-3-7-8-4-...**, where WD+MS is reached during the second mass transfer process. Another possible change of `evol_type` through the volution is **...-3-7-8-7-8-4-...**, which will be mentioned in the next paragraph. Statistically, we found that **(***TO-DO***)** fraction of all our 320000 simulated binaries experience two CE processes before reaching WD+MS. To explain this qualitatively, we notice that when the primary loses too much mass during the first CE, the CE process ends, as the radius of the primary becomes smaller than the Roche lobe. After the primary fills its Roche lobe and has a large enough envelope again, the CE process resumes and causes two CE processes in total.

From Figure 1, we also notice that final separation a_f jumps obviously at about $2.9\,\mathrm{au}$, and $7.1\,\mathrm{au}$. After investigating the `bpp` array of these simulations, we find out the jump at about $2.9\,\mathrm{au}$ and $7.1\,\mathrm{au}$ is likely due to the difference of `kstar_1` at the start of RLOF. For $a_i < 2.9\,\mathrm{au}$, RLOF starts when `kstar_1 = 3`. For $a_i = 2.9\,\mathrm{au}$, RLOF starts when `kstar_1 = 4`. For $2.9\,\mathrm{au} < a_i < 7.1\,\mathrm{au}$, RLOF starts when `kstar_1 = 5`. For $a_i > 7.1\,\mathrm{au}$, RLOF starts when `kstar_1 = 6`. For different star type, the structure and mass of the envelope is different, leading to different binding energy E_{bind} and thus different final separation a_f.

Inspecting more closely, we found that the final separation a_f jumps at about $5.2 \sim 5.4\,\mathrm{au}$. This is especially obvious with $\alpha_{\mathrm{CE}} = 0.3$. To illustrate, we zoom in the simulation results of $\alpha_{\mathrm{CE}} = 0.3$, and present the change of final separation a_f as initial separation a_i increases in Figure 2. From here, we can clearly see two jumps — one between $5.1\,\mathrm{au}$ and $5.2\,\mathrm{au}$, the other at $5.34\,\mathrm{au}$. To explain this, we

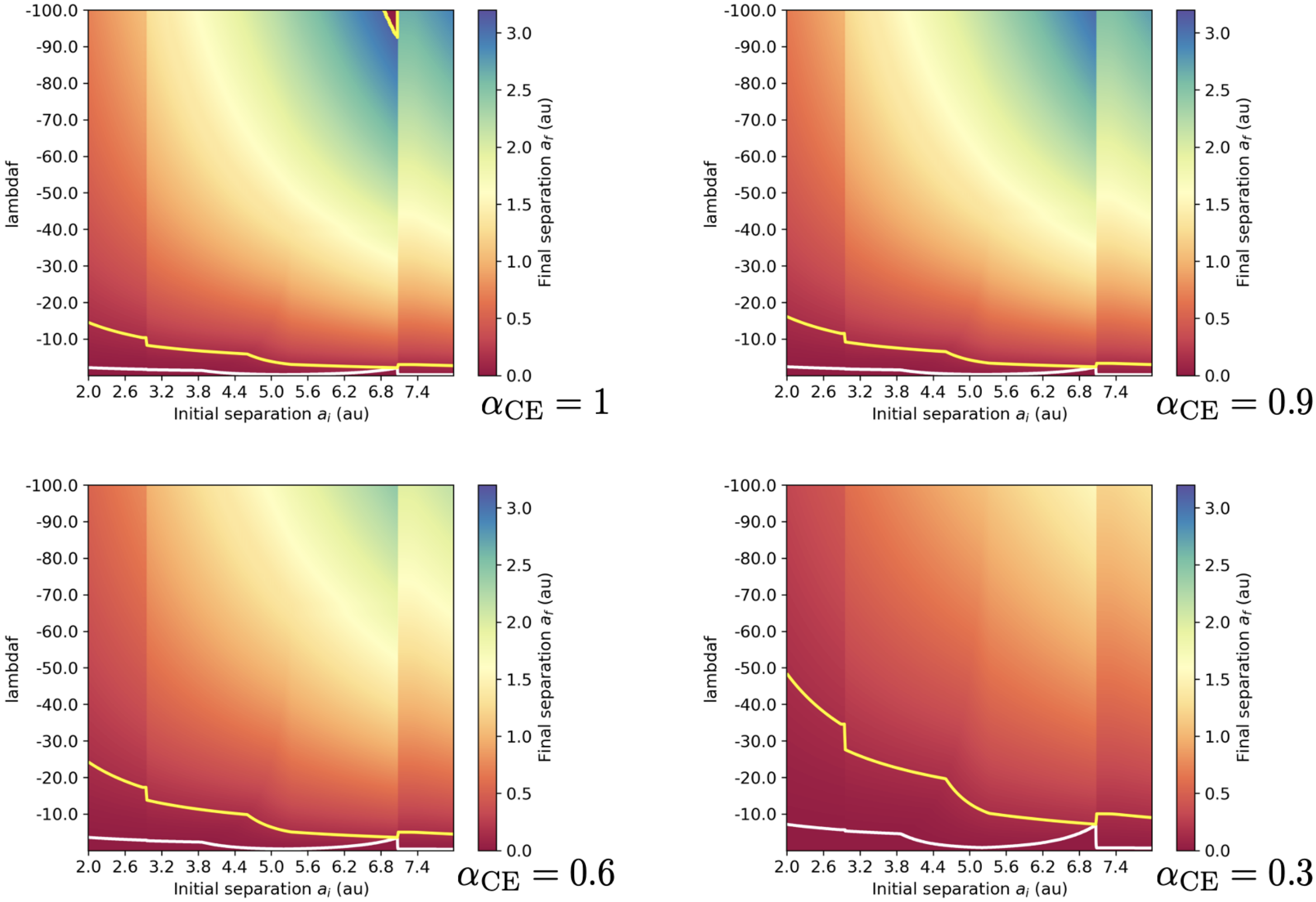

Figure 1: Heat map of final separation a_f against initial separation a_i and CE flag $-\lambda$. Different panels represent four different CE efficiencies $\alpha_{\rm CE} = 1$, 0.9, 0.6, and 0.3. The white and yellow contour corresponds to $a_f = 0.01\,{\rm au}$ and $a_f = 0.15\,{\rm au}$ respectively. WD+MS binaries is not possible for separation smaller than 0.01 au, and 0.15 au is the minimum separation of wide WD+MS binaries in observational results. Outside the white contour no desired system forms.

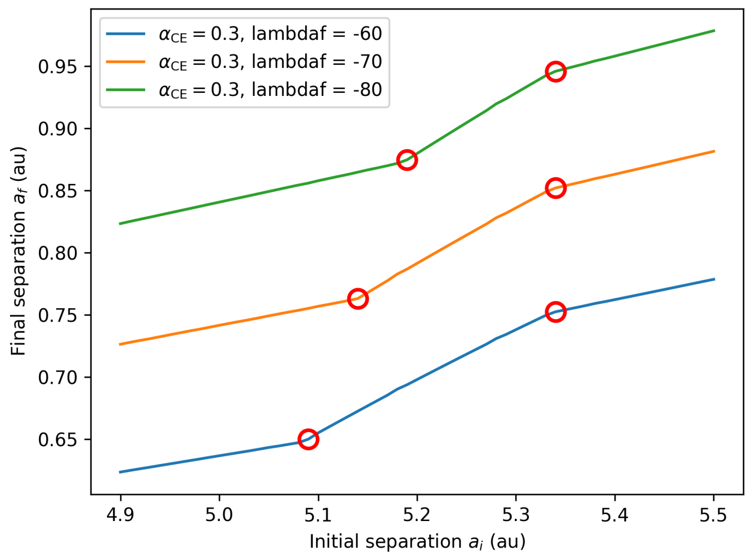

Figure 2: Dependence of final separation a_f on initial separation a_i for $\alpha_{\rm CE} = 0.3$. Simulation results of $\lambda_f = 60$, 70, and 80 are shown. The red circles emphasizes the jump of final separation as initial separation increases.

again go to the `bpp` array of these systems. The first jump is because the evolution process changes from **3-7-8-4-3-7-8-4** to **3-7-8-7-8-4**. This means that for relatively larger initial separation a_i, the primary fills its Roche lobe all the time, leading to more mass loss during a shorter timescale and thus larger final separation. For the second jump, it is because `kstar_1` changes from `8` to `9` at the start of the second common envelope. This changes the binding energy of the common envelope and thus changes the final separation.

Finally, notice that there exists a small triangular gap in the figure for $\alpha_{\rm CE} = 1$. This is because `kstar_1` becomes a neutron star and no rows in the `bpp` gets selected.

In conclusion, with a large λ, it is possible to create wide post-mass transfer WD+MS systems with final separation $a_f > 0.15\,\mathrm{au}$, which is the minimal separation of our observed objects. In next section, we will compare these results with default settings in COSMIC and with results in [Yamaguchi et al., 2024a], in order to investigate the possibility of forming wide WD+MS systems through CE.

2.1.3 Comparison

After we have obtained the simulation results for different initial conditions, now we can calculate the effective λ that matches with results in [Yamaguchi et al., 2024a]. For each fixed initial separation a_i, we loop through the COSMIC results with the same initial separation, and find the λ value that results in a final separation closest to MESA model results. We record this λ as the effective λ that matches the binding energy formalism at initial separation a_i.

We present the fitting results for energy budget $E_{\rm bind} = E_{\rm grav} + E_{\rm int}$ in Figure 3. Notice that in the central panel, there is a small bump of the blue line. This is because at $6 \sim 7\,\mathrm{au}$, we cannot reach such low final separation in COSMIC while forming a WD+MS binary at the same time. From the left panel, we can see that it is possible to create WD+MS binaries with $a_f > 0.15\,\mathrm{au}$ in MESA as long as internal energy $E_{\rm int}$ is included, with initial separation $a_i > 3.5\,\mathrm{au}$. However, in the right panel we show

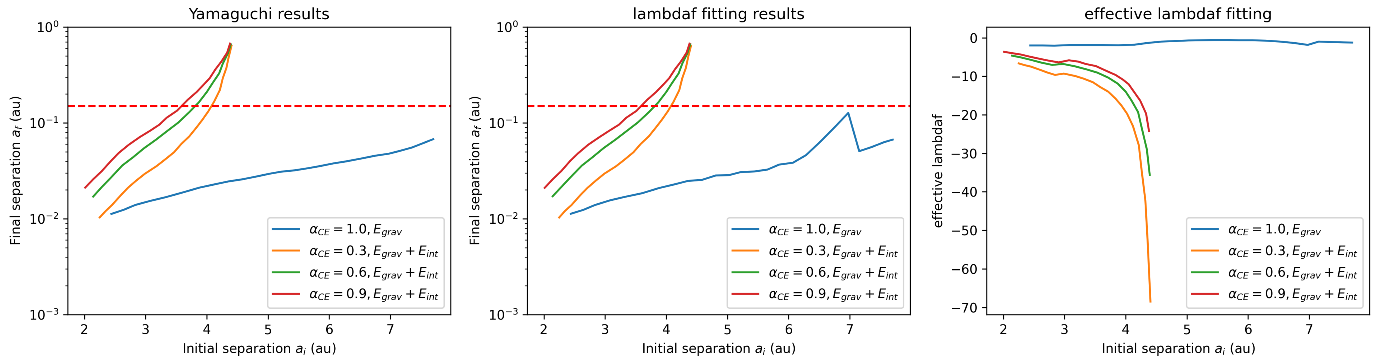

Figure 3: Effective λ fitting results of a $7\,\mathrm{M}_\odot + 1\,\mathrm{M}_\odot$ system for common envelope structure in MESA. Different lines represent different α_{CE} and different common envelope energy budget, as shown in the legend. Left panel: recreation of MESA results in [Yamaguchi et al., 2024a] of how final separation a_f depends on initial separation a_i. Central panel: COSMIC results of how final separation a_f depends on initial separation a_i, produced by the effective λ calculated. Right panel: effective λ in COSMIC that corresponds to the MESA results for each initial separation a_i. The red dashed line in the left and middle panel represents 0.15 au, which is the minimal separation for observed wide post-CE WD+MS binaries.

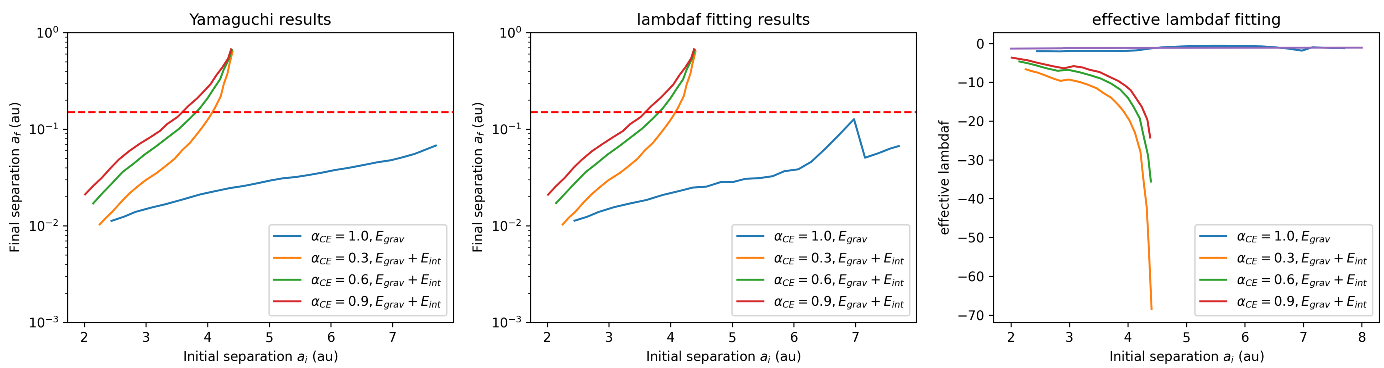

Figure 4: Same as Figure 3, but with default λ in COSMIC model included in the right panel with the purple line.

that this correspond to very large λ in COSMIC ($\lambda >\sim 20$).

To further compare with the default λ value in COSMIC, we include in the right panel an extra line which represents the default λ value in COSMIC. This default λ in the COSMIC model is calculated following Appendix A of [Claeys et al., 2014]. For all of our case, we have $M_{\mathrm{env}} > 1$. The results is shown in Figure 4. Notice that the default λ value is at order ~ 1, far smaller than the effective λ needed to recreate results in [Yamaguchi et al., 2024a]. Hence, we conclude that in COSMIC, it is not practical to form wide high mass WD+MS system through common envelope processes, since the required λ is too large.

In Figure 5, we present the same results for another energy budget of the CE process. Rather than including both thermal and recombination energy into the binding energy, we use two coefficients α_{th} and α_{rec} to consider their contribution to E_{bind} separately. That is,

$$E_{\mathrm{bind}} = E_{\mathrm{grav}} + \alpha_{\mathrm{th}} E_{\mathrm{th}} + \alpha_{\mathrm{rec}} E_{\mathrm{rec}}.$$

We notice that the effective λ now gets with in the order of ~ 10. However, none of these initial separation and λ results in wide WD+MS system with final separation $a_f > 0.15\,\mathrm{au}$. Therefore, we conclude that with the new energy budget, it is not practical to form wide WD+MS binaries either.

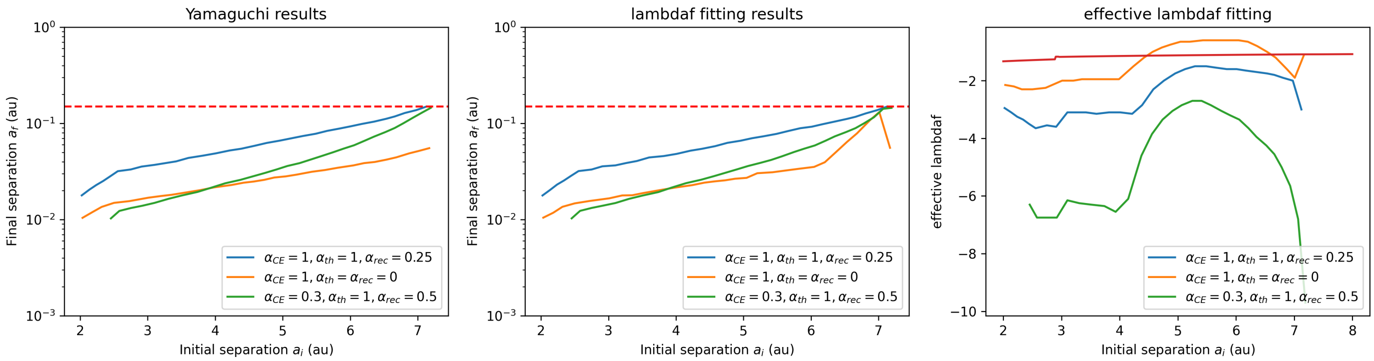

Figure 5: Same as Figure 4, but with a different common envelope energy budget. For results shown in these figures, $E_{\text{bind}} = E_{\text{grav}} + \alpha_{\text{th}} E_{\text{th}} + \alpha_{\text{rec}} E_{\text{rec}}$, where the coefficients α_{th} and α_{rec} for different line is shown in the legend. The red line in the right panel indicates default λ in COSMIC.

2.2 Low Mass Systems ($1.5\,\mathrm{M}_\odot + 0.85\,\mathrm{M}_\odot$)

2.2.1 Methods and results

According to [Yamaguchi et al., 2024b], the WD mass in the Gaia sample ranges from $0.5\,\mathrm{M}_\odot$ to $0.8\,\mathrm{M}_\odot$, which corresponds to progenitor mass of $1\,\mathrm{M}_\odot$ to $3\,\mathrm{M}_\odot$. The companions mass has a median of $0.85\,\mathrm{M}_\odot$. MESA results for $1.5\,\mathrm{M}_\odot + 0.85\,\mathrm{M}_\odot$ systems is documented in [Yamaguchi et al., 2024a]. Hence, we consider a $1.5\,\mathrm{M}_\odot + 0.85\,\mathrm{M}_\odot$ evolution model in COSMIC and compare the results with those in [Yamaguchi et al., 2024a]. For the common envelope, we include all thermal energy E_{th} into the binding energy E_{bind}, while the recombination energy E_{rec} is included in part with a parameter α_{rec}. That is,

$$E_{\text{bind}} = E_{\text{grav}} + E_{\text{th}} + \alpha_{\text{rec}} E_{\text{rec}}.$$

We take the same approach as high mass systems to investigate the effective value of λ in COSMIC that matches with the results in MESA. The initial separation is a linear grid in range $0.5 \sim 6\,\text{au}$ with 400 points. The CE flag `lambdaf` is a linear grid in range $0 \sim -100$ with 2000 steps, which corresponds to $0 \sim 100$ for CE parameter λ. Also, we ran these parameters with four different CE efficiencies — $\alpha_{\text{CE}} = 1$, $\alpha_{\text{CE}} = 0.9$, $\alpha_{\text{CE}} = 0.6$, and $\alpha_{\text{CE}} = 0.3$, the same as recorded in [Yamaguchi et al., 2024b]. In total, for each of the 4 different CE efficiency α_{CE}, we ran a grid of 80000 binary star systems with different initial separation a_i and CE parameter λ.

After simulation is finished, we again select the time-step when the system finished CE for the first time, and record the final separation if the system is a desried WD+MS system. The result is presented in Figure 6.

To compare the results with [Yamaguchi et al., 2024b], we use the same approach as that for high mass systems. In Figure 7, we compare COSMIC with MESA model that includes binding energy of the entire envelope. In Figure 8, we compare COSMIC with MESA model that includes only binding energy of the outer envelope. Notice that we do not have fitting results for $a_i > 4\,\text{au}$. This is because no WD+MS binaries form in COSMIC for such initial separation range.

From the left panel of Figure 7, we can see that wide WD+MS systems can form in MESA model when $a_i > 2.5\,\text{au}$. This is reproduced in COSMIC with $\lambda \sim 1$.Hence, wide WD+MS can form for $a_i > 2.5\,\text{au}$ with parameter λ about the same as default. Recall that for high mass system, wide WD+MS systems cannot form without $\lambda \sim 10^2$. This is a significant difference between high mass systems and low mass systems.

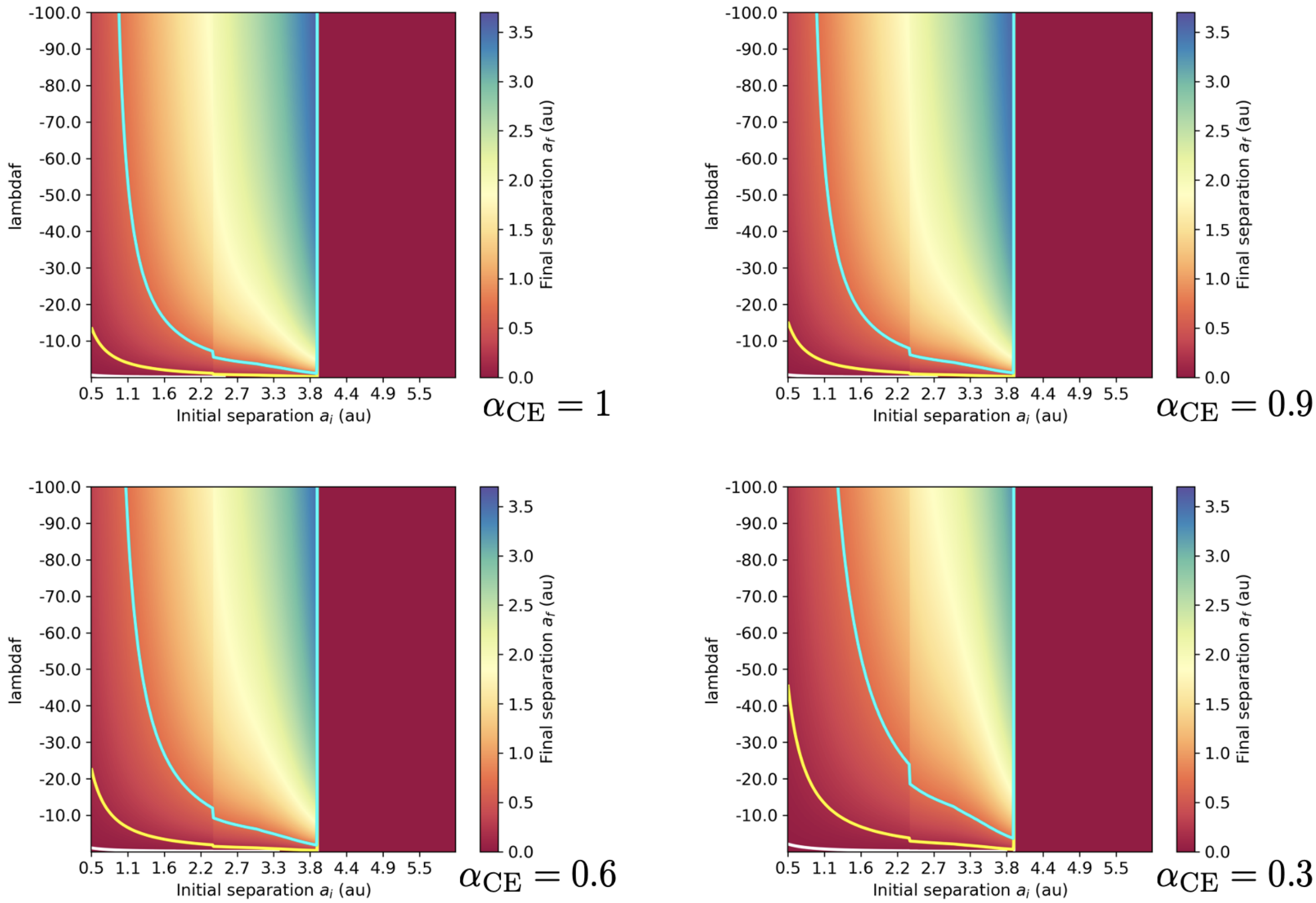

Figure 6: Heat map of final separation a_f against initial separation a_i and CE flag $-\lambda$. Different panels represent four different CE efficiencies $\alpha_{\rm CE} = 1$, 0.9, 0.6, and 0.3. The white and yellow contour corresponds to $a_f = 0.01\,$au and $a_f = 0.15\,$au respectively. WD+MS binaries is not possible for separation smaller than 0.01 au, and 0.15 au is the minimum separation of wide WD+MS binaries in observational results. Outside the white contour no desired system forms.

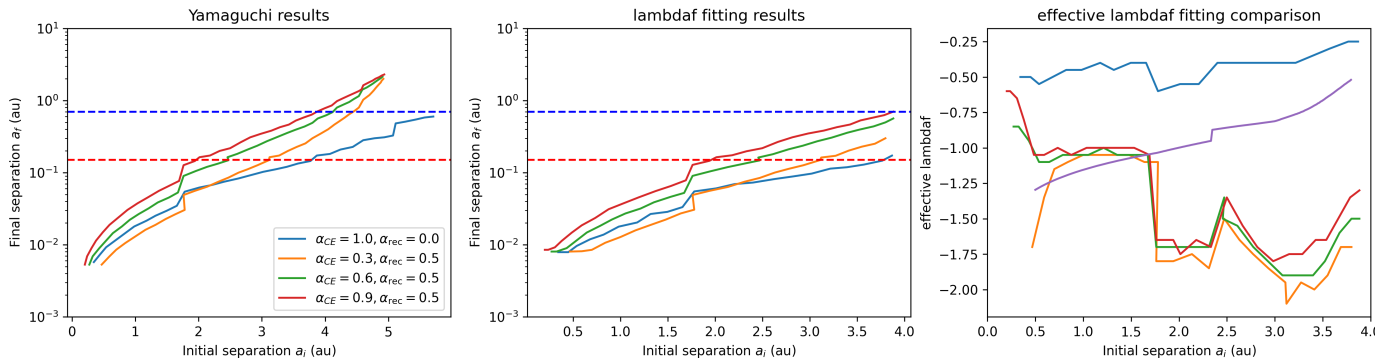

Figure 7: Effective λ fitting results of a $1.5\,\mathrm{M}_\odot + 0.85\,\mathrm{M}_\odot$ system for common envelope structure in MESA. Binding energy of the *entire envelope* is considered. Left Panel: MESA results in [Yamaguchi et al., 2024b] of how final separation a_f depends on initial separation a_i. Central Panel: COSMIC results of how final separation a_f depends on initial separation a_i, produced by the effective λ. Right Panel: effective λ in COSMIC that corresponds to the MESA results for each initial separation a_i. The purple line represents default λ calculated using [Claeys et al., 2014]. The red dashed line and the blue dashed line in the left and central panel represents 0.15 au and 0.7 au respectively. 0.15 au is the minimal separation for observed wide post-CE WD+MS binaries, while 0.7 au is the typical separation for wide post-CE WD+MS binaries.

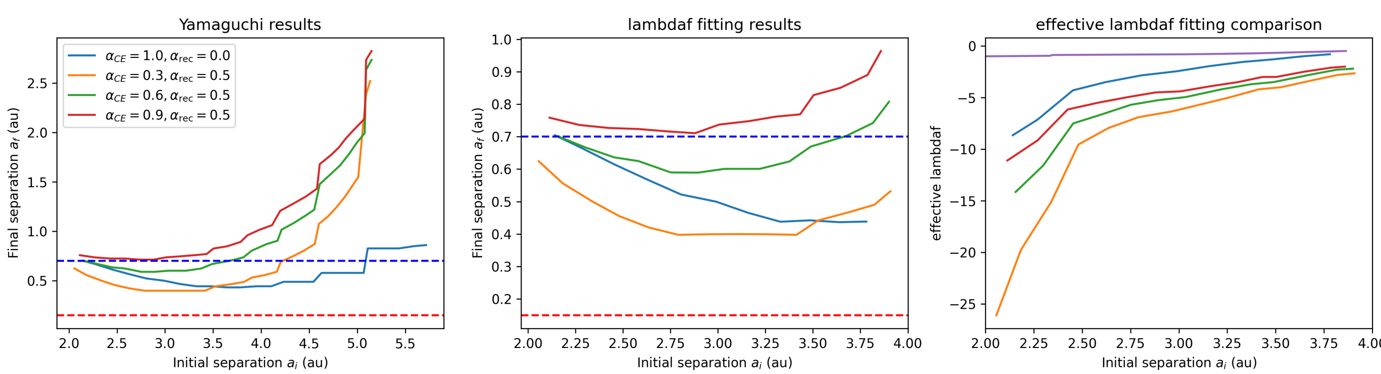

Figure 8: Same as Figure 8 but only binding enregy of the *outer envelope* is considered.

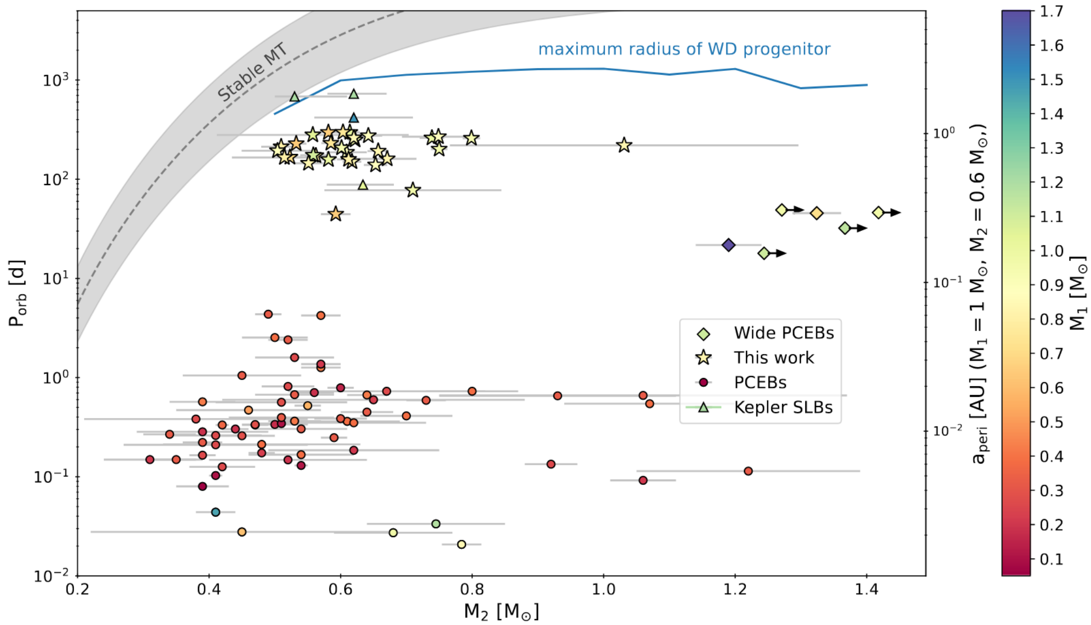

Figure 9: $M_{\rm WD} - P_{\rm orb}$ relation of observed wide post-mass transfer binaries. White dwarf mass $M_{\rm WD}$ correspond to The colors of the points represent the masses of the luminous companion, $M_\star$. On the right axis, we show the minimum orbital separation $a_{\rm peri}$, corresponding to the period assuming companion mass $M_\star = 1\,\mathrm{M}_\odot$ and white dwarf mass $M_{\rm WD} = 0.6\,\mathrm{M}_\odot$. The dashed line and the grey region is the track along which binaries undergoing stable MT are expected to evolve according to [Rappaport et al., 1995]
.

3 Formation Through Stable Mass Transfer

After exploring the formation of WD+MS binaries through common envelope, we investigate the possibility of forming WD+MS binaries through stable mass transfer. In [Yamaguchi et al., 2024b], the author plot the $M_{\rm WD} - P_{\rm orb}$ relation of observed wide WD+MS bianries, and argues that it is not possible to form wide WD+MS binaries through stable mass. The plot is recreated in Figure 9, and from the figure, we can see that the observed wide post-mass transfer WD+MS bianries do not match the theoretical $M_{\rm WD} - P_{\rm orb}$ relation for stable mass transfer calculated in [Rappaport et al., 1995]. Also, the author aruges that stable mass transfer requires donors on SGB at the onset of mass transfer. However, this will not lead to WDs with masses observed [Yamaguchi et al., 2024b].

As in the common envelope section, we investigate how the formation of WD+MS binaries depends on various parameters in high mass systems using $7\,\mathrm{M}_\odot + 1\,\mathrm{M}_\odot$ binaries, and in low mass systems using $1.5\,\mathrm{M}_\odot + 0.85\,\mathrm{M}_\odot$ binaries.

4 Population Synthesis Results

References

[Claeys et al., 2014] Claeys, J., Pols, O., Izzard, R., Vink, J., and Verbunt, F. (2014). Theoretical uncertainties of the type ia supernova rate. *Astronomy & Astrophysics*, 563:A83.

[Rappaport et al., 1995] Rappaport, S., Podsiadlowski, P., Joss, P., Di Stefano, R., and Han, Z. (1995). The relation between white dwarf mass and orbital period in wide binary radio pulsars. *Monthly*

Notices of the Royal Astronomical Society, 273(3):731–741.

[Yamaguchi et al., 2024a] Yamaguchi, N., El-Badry, K., Fuller, J., Latham, D. W., Cargile, P. A., Mazeh, T., Shahaf, S., Bieryla, A., Buchhave, L. A., and Hobson, M. (2024a). Wide post-common envelope binaries containing ultramassive white dwarfs: evidence for efficient envelope ejection in massive asymptotic giant branch stars. *Monthly Notices of the Royal Astronomical Society*, 527(4):11719–11739.

[Yamaguchi et al., 2024b] Yamaguchi, N., El-Badry, K., Rees, N., Shahaf, S., Mazeh, T., and Andrae, R. (2024b). Wide post-common envelope binaries from gaia: orbit validation and formation models. *arXiv preprint arXiv:2405.06020*.